B-IntraSeismic: Uncertainty quantification in seismic inversion via implicit neural representations

J. Romero[1], W. Heidrich[1], M. Ravasi[1,2]

[1] King Abdullah University Of Science And Technology; [2] Shearwater GeoServices

Summary

We present B-IntraSeismic, a Bayesian framework that quantifies uncertainty in seismic inversion by combining variational inference with implicit neural representations. Our approach offers two implementations: BIS, which employs mean-field Gaussian approximation, and BIS-Flow, which captures complex posterior distributions using conditional normalizing flows. Testing on a synthetic dataset demonstrates that both methods generate high-resolution mean models and uncertainty estimates (in the form of standard deviation maps), with BIS-Flow particularly excelling at characterizing multimodal and skewed distributions in complex geological settings. This framework bridges the gap between traditional deterministic inversions and probabilistic approaches, offering a practical solution for large-scale Bayesian seismic inversion.

B-IntraSeismic: Uncertainty quantification in seismic inversion via implicit neural representations

Introduction

Seismic inversion is a critical process in geophysical exploration, enabling the estimation of subsurface properties such as acoustic impedance from post-stack seismic data. However, this process is inherently ill-posed, meaning that multiple solutions can fit the observed data equally well. Consequently, accurately quantifying uncertainty is essential to assess the reliability of the inversion results (Tarantola and Valette, 1981; Ulrych et al., 2001) and to provide geoscientists with a comprehensive understanding of different plausible subsurface configurations. Bayesian seismic inversion addresses this challenge by treating subsurface parameters as random variables with probability distributions and seeking to estimate their posterior distribution conditioned on seismic data. While traditional approaches such as Markov Chain Monte Carlo (MCMC) and Laplace approximations have been widely used, they face significant challenges with scalability and computational cost, especially in large-scale, high-dimensional problems (Mosegaard and Tarantola, 1995; Sen and Stoffa, 1996; Sambridge and Mosegaard, 2002). Variational inference (VI – Jordan et al., 1998; Blei et al., 2017), combined with deep learning techniques, has recently emerged as a promising alternative, offering a balance between computational efficiency and the ability to approximate complex posterior distributions. However, selecting an appropriate proposal distribution remains a critical challenge, as it directly affects the quality of the inferred posterior.

In this study, we extend IntraSeismic, an implicit neural representation (INR)-based framework for seismic inversion (Romero et al., 2024) to the Bayesian setting. More specifically, we introduce B-IntraSeismic, a VI-powered approach for seismic inversion, and propose two variants: B-IntraSeismic (BIS), which employs a mean-field Gaussian approximation for efficient and scalable uncertainty quantification, and B-IntraSeismic with Conditional Normalizing Flows (BIS-Flow), which enhances the flexibility of the mean-field approximation by capturing complex, non-Gaussian posterior distributions. These methods are evaluated on a synthetic dataset demonstrating their ability to produce high-resolution mean models and standard deviation maps while maintaining computational efficiency.

Theory and Methods

The core idea of B-IntraSesimic, as an extension of its deterministic counterpart IntraSeismic, is to approximate the posterior distribution of subsurface acoustic impedance, $\mathbf{m}$, conditioned on post-stack seismic data, $\mathbf{d}$. In the Bayesian setting, the posterior is defined by Bayes' theorem as

$$p(\mathbf{m}|\mathbf{d}) \propto p(\mathbf{d}|\mathbf{m})p(\mathbf{m}), \tag{1}$$

where $p(\mathbf{d}|\mathbf{m})$ and $p(\mathbf{m})$ are the likelihood and prior distributions, respectively. The inversion problem is framed as an optimization task that minimizes the negative of the evidence lower bound (ELBO), defined as:

$$\mathscr{L} = -\mathbb{E}_{q(\mathbf{m})}[\log p(\mathbf{d}|\mathbf{m})] + \mathrm{KL}(q(\mathbf{m})||p(\mathbf{m})), \tag{2}$$

where $q(\mathbf{m})$ is the variational approximation to the true posterior, and KL denotes the Kullback-Leibler divergence. In the specific case of post-stack seismic inversion, when we incorporate Gaussian priors and assume Gaussian noise, we have:

$$\log p(\mathbf{d}|\mathbf{m}) = \frac{1}{2}||\mathbf{d}-\mathbf{Gm}||_2^2, \quad \log p(\mathbf{m}) = \log p_1(\mathbf{m}) + \log p_2(\mathbf{m}) = \frac{\lambda_1}{2}||\mathbf{m}+\mathbf{m}_0||_2^2 + \frac{\lambda_2}{2}||\mathbf{Dm}||_2^2, \tag{3}$$

Where $\mathbf{G}$ is the seismic modeling operator that computes the seismic data from the logarithm of the acoustic impedance model $\mathbf{m}$, which is then compared with the observed data $\mathbf{d}$. The log of the prior distribution $p(\mathbf{m})$ consists of the sum of two log-priors: the first, $\log p_1(\mathbf{m})$, encourages the solution to stay close to a known low-frequency background model $\mathbf{m}_0$, and the second, $\log p_2(\mathbf{m})$, enforces smoothness in the solution, where $\mathbf{D}$ represents the Laplacian operator. The hyperparameters λ_1 and λ_2 control the relative influence of these priors during the inversion process. Note that when a prior covariance matrix is available, it can be incorporated by replacing the isotropic penalty terms with quadratic forms involving the covariance matrix. For example, the term $||\mathbf{m}+\mathbf{m}_0||_2^2$ can be replaced with $(\mathbf{m}+\mathbf{m}_0)^T\Sigma^{-1}(\mathbf{m}+\mathbf{m}_0)$, where Σ is the covariance matrix. This inclusion allows for anisotropic or spatially varying constraints to be directly embedded in the prior.

Two approaches are introduced to parameterize the proposal distribution $q(\mathbf{m})$ in Equation 2: (1) B-IntraSeismic (BIS), which uses a mean-field Gaussian proposal, and (2) BIS-Flow, which employs conditional normalizing flows (CNFs) to capture non-Gaussian characteristics of the posterior, while still being a mean-field approximation. BIS represents the subsurface acoustic impedance as a Gaussian distribution where the parameters (mean and standard deviation) are learned through the non-linear mapping module of IntraSeismic. BIS-Flow extends BIS by incorporating conditional normalizing flows to model non-Gaussian, multimodal, or skewed posterior distributions. The CNF employed in BIS-Flow transforms a base Gaussian distribution into a complex target distribution using invertible mappings conditioned on the INR's output feature vectors. For a transformation f, the flow computes the transformed distribution using the change-of-variables formula:

$$q(\mathbf{m}) = q_0(\mathbf{z}) \left| \det \frac{\partial f}{\partial \mathbf{z}} \right|^{-1}, \tag{4}$$

where $\mathbf{z}$ is sampled from a base Gaussian distribution $q_0(\mathbf{z})$. In this study, we employ Gaussianization flows (Meng et al., 2020), a powerful architecture for mapping non-Gaussian data into a Gaussian distribution.

Results

The Marmousi model (Brougois et al., 1990) served as a synthetic example to evaluate the performance of the proposed Bayesian methods, B-IntraSeismic (BIS) and BIS-Flow, in comparison to analytical and Randomize-Then-Optimize (RTO – Bardsley et al., 2014) solutions. We utilize a smooth version of the Marmousi model as the initial background model for the inversion process (Figure 1b). To generate synthetic post-stack seismic data, we apply the linear post-stack modeling operator to the logarithm of the acoustic impedance model (computed by scaling the provided velocity model by a constant density value) using a 15 Hz peak-frequency Ricker wavelet. The data and wavelet, originally ranging from -1 to 1, are scaled by a factor of 50, and the data is subsequently contaminated with Gaussian noise with a standard deviation of 1.0 (Figure 1c).

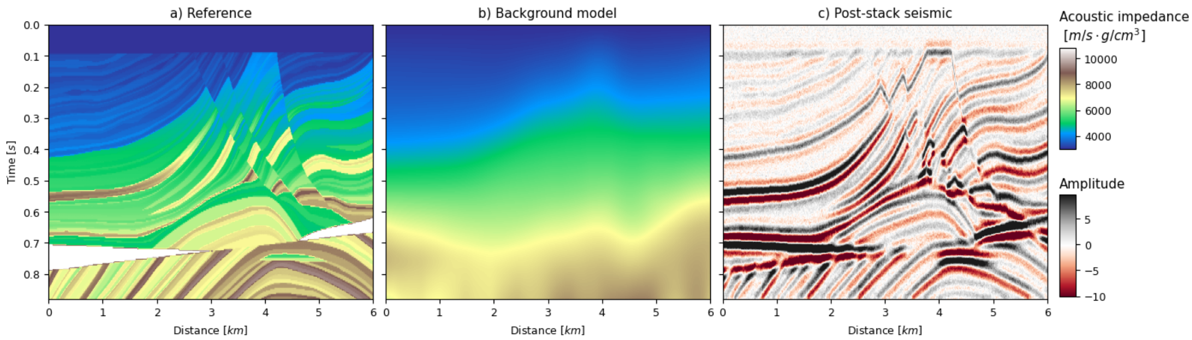

Figure 1 *Marmousi acoustic impedance model used as the reference solution, background model used as the mean for the proximity prior, and post-stack seismic data with added Gaussian noise.*

We use the analytical and RTO solutions as benchmarks for the Bayesian inversion of the synthetic Marmousi seismic data (Figure 2a-d). In both cases, we used the two prior distributions described in Equation 3. The recovered analytical and RTO mean models effectively reconstruct the structural features and impedance values of the ground truth model with a similar signal-to-noise ratio (SNR). The standard deviation for the analytical case exhibits strong structural conformance, with maximum variance corresponding to regions of high impedance contrast. For the RTO method, the standard deviation appears under-determined, likely due to the limited number of realizations (1000 perturbations).

The results obtained with BIS (Figure 2e-f), using the same priors as the analytical case, demonstrate that the predicted mean and standard deviation closely resemble those of the analytical posterior distribution. The mean, despite having a lower SNR, successfully captures the main features of the inverted model, while the standard deviation map exhibits similar conformance and a comparable range of values to those obtained analytically (Figure 2b). For BIS-Flow (Figure 2g-h), we employed a blockiness-promoting prior (similar to TV regularization), which encourages higher-resolution realizations of the

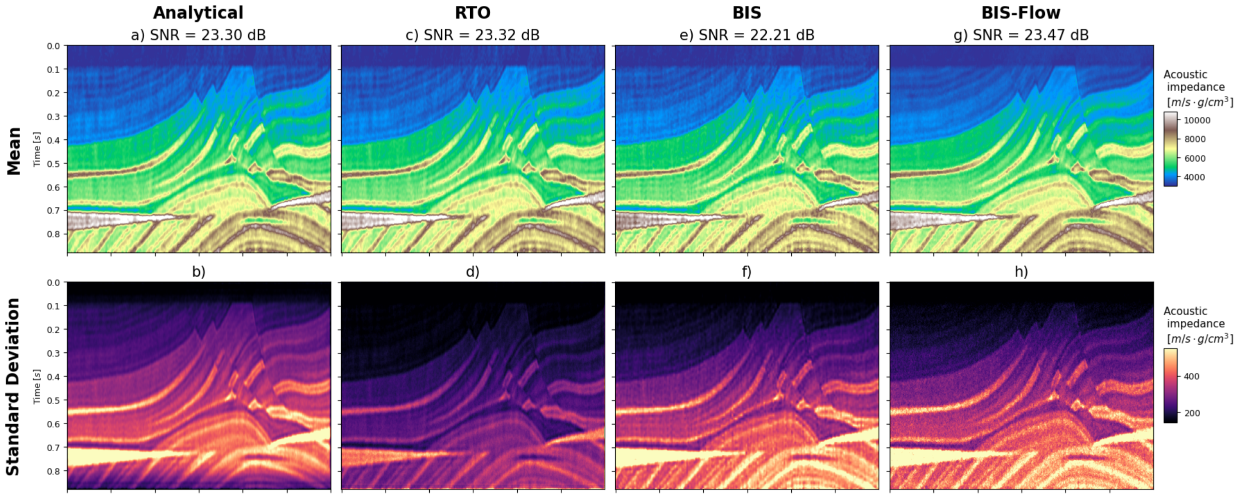

Figure 2 *Comparison of the analytical, RTO, BIS, and BIS-Flow for the Bayesian inversion of the post-stack modeled Marmousi data.*

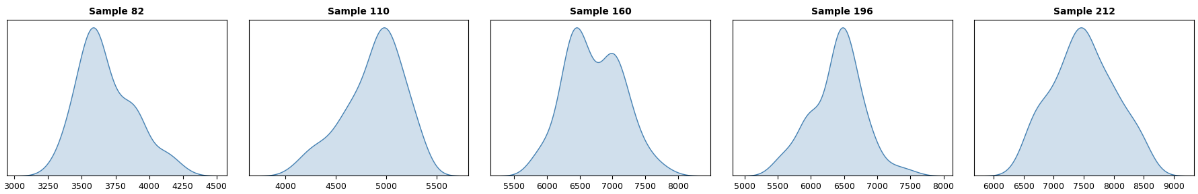

Figure 3 *Kernel density estimation of BIS-Flow predicted proposal distribution samples at 5 random locations.*

posterior distribution. This approach enabled BIS-Flow to achieve the highest SNR for the predicted mean across the methods and a slightly higher resolution in the standard deviation map compared to BIS. While both BIS and BIS-Flow parameterize each point independently, without accounting for joint correlations between different locations in the model, BIS-Flow predicts an unparameterized posterior distribution, making it more robust in capturing complex subsurface features. Figure 3 illustrates the predicted distributions for randomly selected points in the model, revealing that the posterior distributions are notably non-Gaussian.

Figure 4 illustrates the loss and SNR evolution over iterations for both BIS and BIS-Flow corresponding to the results in Figures 2i-j. The loss in both cases exhibits a steep decline during the first 100 iterations, with SNR converging at different points: BIS reaches a plateau after 400 iterations, whereas BIS-Flow converges more quickly, matching the SNR of BIS at 200 iterations and showing a marginal increase until 800 iterations. All experiments are conducted on an AMD EPYC 7713 64-Core Processor equipped with a single NVIDIA TESLA A100.

Conclusions

In this study, we introduced B-IntraSeismic, a Bayesian extension of the IntraSeismic framework for uncertainty quantification in seismic inversion. By leveraging variational inference and implicit neural representations, the proposed methods—BIS and BIS-Flow—produced high-resolution mean models and standard deviation maps at a reasonable computational cost. BIS-Flow, in particular, demonstrated enhanced flexibility by capturing complex, non-Gaussian posterior distributions, making it well-suited for addressing the inherent uncertainties in seismic data. Results on the Marmousi data underscore the scalability and accuracy of these methods. However, the reliance on the mean-field approximation, while computationally appealing, assumes parameter independence, which can result in underestimated uncertainties and the inability to capture important features of the true posterior, such as parameter correlations. Addressing these limitations will be a key focus of future work.

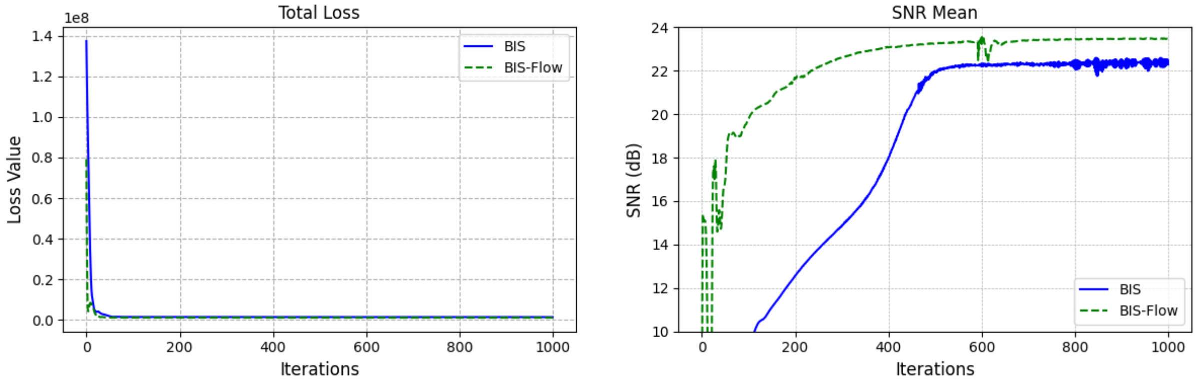

Figure 4 *Loss and SNR of the mean through iterations of BIS and BIS-Flow for the Bayesian inversion Marmousi data.*

References

Bardsley, J.M., Solonen, A., Haario, H. and Laine, M. [2014] Randomize-Then-Optimize: A Method for Sampling from Posterior Distributions in Nonlinear Inverse Problems. *SIAM Journal on Scientific Computing*, **36**(4), A1895–A1910.

Blei, D.M., Kucukelbir, A. and McAuliffe, J.D. [2017] Variational Inference: A Review for Statisticians. *Journal of the American Statistical Association*, **112**(518), 859–877.

Brougois, A., Bourget, M., Lailly, P., Poulet, M., Ricarte, P. and Versteeg, R. [1990] Marmousi, model and data. European Association of Geoscientists & Engineers, cp. ISSN: 2214-4609.

Jordan, M.I., Ghahramani, Z., Jaakkola, T.S. and Saul, L.K. [1998] An Introduction to Variational Methods for Graphical Models. In: Jordan, M.I. (Ed.) *Learning in Graphical Models*, Springer Netherlands, Dordrecht, 105–161.

Meng, C., Song, Y., Song, J. and Ermon, S. [2020] Gaussianization Flows. ArXiv:2003.01941.

Mosegaard, K. and Tarantola, A. [1995] Monte Carlo sampling of solutions to inverse problems. *Journal of Geophysical Research: Solid Earth*, **100**(B7), 12431–12447. _eprint: https://onlinelibrary.wiley.com/doi/pdf/10.1029/94JB03097.

Romero, J., Heidrich, W., Luiken, N. and Ravasi, M. [2024] Seismic Reservoir Characterization With Implicit Neural Representations. *Journal of Geophysical Research: Machine Learning and Computation*, **1**(3), e2024JH000275.

Sambridge, M. and Mosegaard, K. [2002] Monte Carlo Methods in Geophysical Inverse Problems. *Reviews of Geophysics*, **40**(3), 3–1–3–29. _eprint: https://onlinelibrary.wiley.com/doi/pdf/10.1029/2000RG000089.

Sen, M.K. and Stoffa, P.L. [1996] Bayesian inference, Gibbs' sampler and uncertainty estimation in geophysical inversion. *Geophysical Prospecting*, **44**(2), 313–350. _eprint: https://onlinelibrary.wiley.com/doi/pdf/10.1111/j.1365-2478.1996.tb00152.x.

Tarantola, A. and Valette, B. [1981] Inverse problems = Quest for information. *Journal of Geophysics*, **50**(1), 159–170.

Ulrych, T.J., Sacchi, M.D. and Woodbury, A. [2001] A Bayes tour of inversion: A tutorial. *Geophysics*, **66**(1), 55–69.